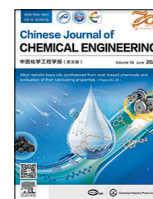




Contents lists available at ScienceDirect

## Chinese Journal of Chemical Engineering

journal homepage: [www.elsevier.com/locate/CJChE](http://www.elsevier.com/locate/CJChE)

## Full Length Article

## Liquid-phase esterification of methacrylic acid with methanol catalyzed by cation-exchange resin in a fixed bed reactor: Experimental and kinetic studies

Junyang Liu<sup>1,2</sup>, Luming Wang<sup>1,2</sup>, Yuhang Bian<sup>2</sup>, Chunshan Li<sup>1,2,3</sup>, Zengxi Li<sup>1,\*</sup>, Jie Li<sup>2,\*</sup><sup>1</sup> School of Chemical Sciences, University of Chinese Academy of Sciences, Beijing 100049, China<sup>2</sup> Beijing Key Laboratory of Ionic Liquids Clean Process, Key Laboratory of Green Process and Engineering, State Key Laboratory of Multiphase Complex Systems, Institute of Process Engineering, Chinese Academy of Sciences, Beijing 100190, China<sup>3</sup> Langfang Technological Center of Green Industry, Langfang 065801, China

## ARTICLE INFO

## Article history:

Received 28 April 2022

Received in revised form 10 October 2022

Accepted 16 October 2022

Available online 8 November 2022

## Keywords:

Kinetics

Esterification

Methyl methacrylate

Cation-exchange resin

Fix bed reactor

## ABSTRACT

The kinetic behavior of esterification between methacrylic acid and methanol catalyzed by NKC-9 resin was studied in a fixed bed reactor. The reaction was conducted in the temperature range of 323.15 to 368.15 K with the molar ratio of reactants from 0.8 to 1.4 under certain pressure. The measurement data were regression with the pseudo-homogeneous (P-H), Eley-Rideal (E-R), and Langmuir-Hinshelwood (L-H) heterogeneous kinetic models. Independent adsorption experiments were implemented to gain the adsorption equilibrium constants of four components. Among the above three models, the L-H model exhibited the best fitting results. The stability of NKC-9 was evaluated by long-term running with the yield of methyl methacrylate no decrease during 3000 h operation. The structure and physicochemical properties of the new and used catalyst were performed by several characterizations including thermogravimetric analysis (TG), scanning electron microscope (SEM), X-ray diffraction (XRD) and Fourier transform infrared spectroscopy (FT-IR) and so on.

© 2022 The Chemical Industry and Engineering Society of China, and Chemical Industry Press Co., Ltd. All rights reserved.

## 1. Introduction

Methyl methacrylate (MMA), an essential organic chemical product and synthetic methyl poly-methacrylate (PMMA) monomer, is widely used in the production of surface coating, automotive parts, and modifier for PVC [1–3]. The copolymers of MMA were also utilized to manufacture lighting equipment, membrane and transparent plastic as a result of the characteristics of good transparency, excellent electrical performance and weather resistance. The market requirements for MMA have expected steady growth with the increasing demand for organic glass, adhesives and construction industries [4,5].

The fabrication of MMA was industrialized for the first time since the early 20th century. Traditionally, the acetone cyanohydrin (ACH) route was adopted by most manufacturers to produce MMA [6]. Nevertheless, the usage of the highly toxic cyanide and corrosive concentrated sulfuric acid in the ACH route was unsustainable and environmentally unfriendly. In order to replace the

acetone cyanohydrin strategy, a series of industrial production methods of MMA have emerged, such as isobutylene or tert-butanol oxidation process, ethylene carbonylation pathway, and aldol condensation route [7,8]. Among them, the method of aldol condensation suffers from the problem of rapid catalyst deactivation and high energy consumption although it has the advantages of a wide source of raw materials and short process [6,9,10]. Therefore, the ethylene method and isobutylene oxidation are still the main production route, which both contain the process of producing MMA by esterification [11–13]. Inorganic acids, acidic ionic liquids, and solid acids could be used as catalysts in homogeneous or heterogeneous systems [14,15]. The equipment corrosion, difficulty in separation and a large amount of waste were the main problems with homogeneous catalysts such as sulfuric acid and hydrochloric [16–18]. With view to these problems, several heterogeneous catalysts including zeolite [19], functional clay [20], sulfated metal oxide [21,22], poly acid ionic liquid [23], ion-exchange resin [24,25] had been developed.

Ion-exchange resins are of great promise because it has superiority in catalytic ability, cost, separation and recovery, which makes it suitable for long-term operation in industrial application

\* Corresponding authors.

E-mail addresses: [lizengxi@ucas.ac.cn](mailto:lizengxi@ucas.ac.cn) (Z. Li), [lijiequst@ipe.ac.cn](mailto:lijiequst@ipe.ac.cn) (J. Li).

[26–28]. The kinetic behavior of the esterification was often studied for the purpose of implementing the process simulation to facilitate the design of the reactor in real industrial practice [29,30]. According to reports, various cation exchange resins were used to study the kinetic and thermodynamic in batch reactor [31–36]. Nonetheless, there are some disadvantages such as high energy consumption, difficulty in reuse, and are inconsistent with industrial production in a stirred tank reactor. Therefore, the research of kinetic parameters on a fixed bed reactor is necessary for the actual industrial process [37]. In Cheng *et al.*'s work, the kinetic parameters of free fatty acid with methanol on NKC-9 were studied to illustrate the impact of the height of catalyst loading to the conversion of reactants in three scales of fixed bed reactors, and fitted with the P-H model [38]. Russo *et al.* investigated the kinetics of the heterogeneous esterification in the presence of Amberlite IR120 from intermittent to continuous unit [39]. Chen *et al.* reported a novel intensified fixed bed reactor (IFBR) for solving the channel flow problems caused by slow velocity in conventional fixed bed, and the UNIFAC model was used in order to remove the system non-ideality [40]. The author proved that the Langmuir–Hinshelwood–Hougen–Watson (LHHW) model has the best results. With regard to the actual industrial production process, it is necessary for the study of kinetic of catalyst in the continuous reactor. Therefore, the synthesis of MMA through esterification catalyzed by ion exchange resin using a fixed bed reactor was carried out in our work and the lifetime of catalyst was also assessed.

In this study, in order to achieve a continuous reaction process, the method of pressurization was adopted to ensure that the esterification on resin catalysts is in the liquid phase to avoid MMA polymerization during phase transition. Six parameters (the type of resin, catalyst loading, reaction pressure, molar ratio of methanol (MeOH) to MAA, reaction temperature and catalyst stability) were taken into consideration. The adsorption equilibrium constants of non-reactive two substances were obtained and fitted with the data of adsorption experiments. Three models (P-H, E-R and L-H models) were correlated with kinetic data. Long period evaluation experiments were performed and a series of characterizations (XRD, SEM, TG and FT-IR) were adopted to investigate the properties of catalyst before and after use.

## 2. Experimental

### 2.1. Materials

#### 2.1.1. Chemicals

Methacrylic acid (>99.0%), methyl methacrylate (>99.0%), and polymerization inhibitor hydroquinone (>99.0%) were manufactured by Tianjin Damao Chemical Reagent Co. Ltd. (China). Methanol (>99.5%) was obtained from Jinan Colorful Chemical Co. Ltd. (China). All of the above reagents are analytical grades without ulteriorly purification.

#### 2.1.2. Catalysts

NKC-9 catalyst was gained from Tianjin Damao Chemical Reagent Co. Ltd. (China). 001–7 and D001 were fabricated by Tianjin Xinyue Huamei Environmental Protection Technology Co. Ltd. (China). Amberlite IR120 was manufactured by Rohm and Haas (USA). The resin needs to be pretreated before being loaded into the reactor to remove impurities attached to the surface of catalysts. The pretreatment steps are as follows: First of all, resins were vacuum dried at 80 °C for 12 h. It will be soaked and washed with deionized water and methanol respectively until washing solution is clear and transparent after cooling to room temperature, and then the catalysts are stored in methanol solution for later use.

The relevant characteristics of above resins given by the manufacturer were summarized in Table 1.

### 2.2. Experimental apparatus and procedure

#### 2.2.1. Apparatus of esterification and experimental process

As shown in Fig. 1, the synthesis of MMA through esterification was operated in a continuous fix-bed reactor with a height of 50.0 cm and inner diameter of 2.3 cm packed with resin catalyst. For the purpose of guaranteeing the temperature inside the pre-heat tube and reactor, circulating hot oil was applied to heat and the actual temperature was measured by thermocouples. Nitrogen was pumped into the reactor to ensure reaction pressure of the reaction system in the liquid.

The specific operation process was as follows: Firstly, the reaction raw materials were prepared and mixed in a certain proportion and stored in feed tank (1). Pretreated catalyst was packed in the constant temperature section of the reactor. Then, the reactants were continuously transported to the preheating tube for preheating (3) by the advection pump (series II, PEEK; uncertainty of flow rate is 0.001), and reaction was then carried out in the reactor (5). The conditions at different retention times were measured by varying the flow rates in range of 0.2–3.3 ml·min<sup>−1</sup>. Finally, the product mixture was cooled in the liquid storage tank (6) by circulating water bath and collected from the storage tank into a sample bottle at different flow rates. The pressure of reaction system is controlled by the back pressure valve (7) during the reaction. The samples were collected by a syringe and tested on GC at regular intervals. The catalytic reaction of MAA with MeOH on NKC-9 was studied at different reaction conditions and summarized in Table 2.

#### 2.2.2. Adsorption experiments

Adsorption equilibrium constants of liquid were demanded for the heterogeneous kinetic models. According to the experiment method proposed by Song *et al.* [41], binary adsorption experiments were performed. Among the four pairs non-reactive binary components, three pairs (1) MAA with H<sub>2</sub>O, (2) MeOH with MMA, (3) MeOH with H<sub>2</sub>O were investigated. The volume of the adsorption chamber was 30 ml and the temperature of it was determined by the mercury thermometer. 5 g of dried NKC-9 and different concentrations of binary non-reactive solution were placed into the chamber. The heavier component was added first during the solution preparation to decrease the effect of evaporation. The binary mixture on the NKC-9 were adsorbed at 25 °C for 12 h and adsorption liquid were tested at least three times by GC and moisture titrator in each run.

#### 2.2.3. Swelling experiments

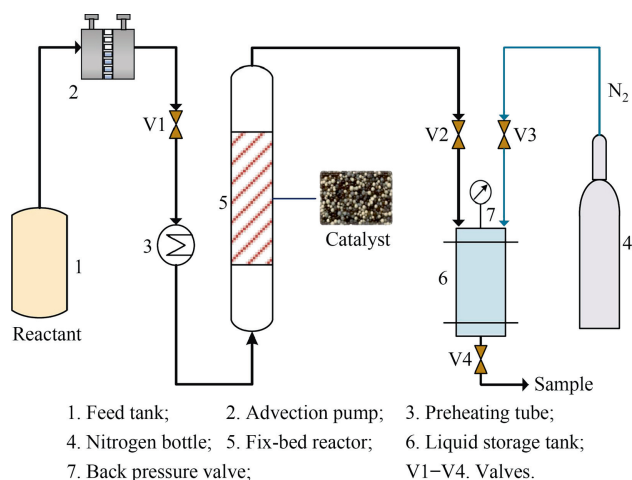
The swelling effect of resin is a key factor for fixed-bed reactors. The swelling ability of NKC-9 on single substance of reaction system was acquired at room temperature in a graduated cylinder with volume of 20 ml. A certain amount of single solution and 5 g of NKC-9 vacuum-dried at 80 °C were added into the graduated cylinder simultaneously. The swelling volume of catalyst was observed after 24 h. At least three experiments were repeated so as to promote the accuracy of the measurement [33].

### 2.3. Quantitative and characteristic analysis

Collected samples periodically were conducted on gas-chromatography (GC-2030, Shimadzu, Japan) equipped with FID detector and capillary column of WondaCap Wax (30 m × 0.25 mm × 0.25 μm). The isobutanol was used as internal standard to calculate the conversion of MAA and selectivity of MMA. Besides, the water content in samples was confirmed by the Karl Fischer

**Table 1**  
Physicochemical properties of four resins

Physical property	Matrix type	Polymer type	Ionic form	Functional group	Exchange capacity/mmol·g <sup>-1</sup>		Moisture content/%	Max operating temperature/°C	Apparent/g·ml <sup>-1</sup>
					dry	wet			
NKC-9	Styrene-DVB	Macro reticular	H <sup>+</sup>	Sulfonic acid	≥4.7	≥1.5	51–59	120	0.75–0.82
001-7		Gel			≥4.5	≥1.9	46–52	100	0.73–0.83
D001		Macro reticular			≥4.8	≥1.6	50–60	100	0.75–0.85
Amberlite IR120		Gel			≥4.4	≥1.8	53–58	120	—

**Fig. 1.** Device diagram of the reactor.

moisture titrator (MA-1, Shanghai Benang Scientific Instrument Co. Ltd. China).

The formula of MAA conversion ( $X_{\text{MAA}}$ ) and MMA selectivity ( $S_{\text{MMA}}$ ) were exhibited in Eqs. (1) and (2), where  $n_{\text{MAA},0}$  and  $n_{\text{MAA},t}$  denote the molar number of MAA at the beginning and after  $t$  time, respectively. And  $n_{\text{MMA},t}$  refers to the number of moles of MMA after  $t$  time.

$$X_{\text{MAA}} = \frac{n_{\text{MAA},0} - n_{\text{MAA},t}}{n_{\text{MAA},0}} \times 100\% \quad (1)$$

$$S_{\text{MMA}} = \frac{n_{\text{MMA},t}}{n_{\text{MAA},0}} \times 100\% \quad (2)$$

**Table 2**  
Experimental conditions of the esterification of methacrylic acid with methanol

Test	$T/K$	$P/\text{MPa}$	MeOH/MAA	Size/mm	$V_{\text{cat}}/\text{ml}$	Retention time/min
1	323.15	0.3	1.0	0.55–0.83	50	0–100
2	338.15	0.3	1.0	0.55–0.83	50	0–100
3	353.15	0.3	1.0	0.55–0.83	50	0–100
4	368.15	0.3	1.0	0.55–0.83	50	0–100
5	368.15	0.1	1.0	0.55–0.83	50	0–100
6	368.15	0.2	1.0	0.55–0.83	50	0–100
7	368.15	0.5	1.0	0.55–0.83	50	0–100
8	368.15	0.3	0.8	0.55–0.83	50	0–100
9	368.15	0.3	1.2	0.55–0.83	50	0–100
10	368.15	0.3	1.4	0.55–0.83	50	0–100
11	368.15	0.3	1.0	0.83–1.70	50	0–100
12	368.15	0.3	1.0	0.38–0.55	50	0–100
13	368.15	0.3	1.0	0.27–0.38	50	0–100
14	368.15	0.3	1.0	0.55–0.83	10	20
15	368.15	0.3	1.0	0.55–0.83	20	40
16	368.15	0.3	1.0	0.55–0.83	30	60
17	368.15	0.3	1.0	0.55–0.83	40	80
18	368.15	0.3	1.0	0.55–0.83	60	120
19	368.15	0.3	1.0	0.55–0.83	70	140

The BET specific surface area and mean pore size of catalyst were verified from nitrogen adsorption–desorption isotherms by a Brunauer–Emmett–Teller (BET) aperture analyzer (ASAP 2460 Micromeritics, USA). The scanning electron microscope (SEM, SU8020, Hitachi, Japan) instrument was adopted to observe the morphologies of NKC-9 sample before and after use. The fresh and used resin were checked on the IR spectra in the range of 500–4000  $\text{cm}^{-1}$  by Thermo Nicolet 8700 spectrometer (USA). X-ray diffraction (XRD) patterns were recorded on the X-ray diffractometer (Smartlab, D/Max-C, Japan) using  $\text{Cu K}\alpha$  source ( $\lambda = 0.154 \text{ nm}$ ). Thermogravimetric measurement of the NKC-9 was conducted on a TGA/DSC analyzer (TG-DTA6300, Japan). The samples were heated from 30 to 900  $^{\circ}\text{C}$  with a heating rate of 10  $^{\circ}\text{C}\cdot\text{min}^{-1}$  in a 30  $\text{ml}\cdot\text{min}^{-1}$   $\text{N}_2$  flow. Elements content of the resin was obtained by an element analyzer (Vario EL cube, Germany).

### 3. Results and Discussion

#### 3.1. Catalyst selecting

Four resins (NKC-9, Amberlite IR120, 001-7 and D001) were performed for preliminary comparison, which was shown in Fig. S1 (Supplementary Material). It could be seen that the addition of the catalyst can significantly increase the reaction rate. Wherein, NKC-9 exhibited the best catalytic performance compared with other resins. Based on the experimental results, the NKC-9 was selected for the following reaction.

#### 3.2. Mass transfer resistance experiments

In order to avoid the distinction of measurement data and regression results, the diffusion limitations of internal and external

on esterification were necessary to be excluded before developing the kinetic experiments.

Wherein, the retention time  $\tau$  of reactants with catalysts can be defined as [29]:

$$\tau = V/F \quad (3)$$

For the purpose of eliminating the effect of external diffusion in the experiment process, it is needed that maintain a certain residence time ( $\tau = 100$  min in our experiments) by changing the feed flow rate and catalyst volume simultaneously to investigate the velocity of reactants passing through the catalyst bed on the impact of the conversion of MAA. When the MAA conversion is not affected by feed flow rate, the external diffusion can be deemed as eliminated.

As shown in Fig. 2, the MAA conversion was independent of enhanced feed flow rate over  $0.4 \text{ ml}\cdot\text{min}^{-1}$ , it is indicated that the influence of the external diffusion can be ignored in this situation.

Screening NKC-9 into different particle sizes (from 0.27 to 1.70 mm) to observe the influence of internal diffusion. Hereon, the reaction was carried out at the same conditions. It could be seen that the catalyst size does not have a significant influence on the conversion of MAA from Fig. 3, it implies that the influence of internal diffusion can be ignored. The experimental results show the conversion of MAA cannot be impacted by catalyst particle size and was consistent with the phenomenon found by Tsai *et al.* [42]. According to BET and BJH models, the values of specific surface area and mean pore diameter were  $6.41 \text{ m}^2\cdot\text{g}^{-1}$  and  $29.92 \text{ nm}$  determined by  $\text{N}_2$  adsorption and desorption method, respectively. And the data of mercury penetration method show that the total pore area of NKC-9 was  $29.11 \text{ m}^2\cdot\text{g}^{-1}$  and the average pore size was  $44.89 \text{ nm}$  [25,36]. The results could be available from Fig. S2, Fig. S3 and Fig. S4.

Therefore, the kinetic studies can be performed at the volume flow rate of  $0.5 \text{ ml}\cdot\text{min}^{-1}$  and catalyst particle size of 0.55 to  $0.83 \text{ mm}$ .

### 3.3. Optimization of conditions and kinetic experiments

#### 3.3.1. Effect of catalyst filling

The influence of the filling amount of catalysts on the conversion of MAA was estimated by changing the filling volume of catalyst ( $V$ ) under the condition of constant feed flow rate of the feed ( $F$ ) is  $0.5 \text{ ml}\cdot\text{min}^{-1}$ . The conversion of MAA increased with the catalyst volume of filling when the catalyst loading is less than 40 ml according to Fig. 4. However, it was nearly identical when the catalyst bed volume exceeds 40 ml. In addition, the selectivity of MMA was above 99% on average and no byproducts were detected.

#### 3.3.2. Effect of reaction pressure

MMA is prone to polymerize at high temperature, thus a certain amount of polymerization inhibitor must be added in the industrial production. Although the conversion of MAA significantly increased when the temperature of reaction system is lift, the vaporization of MMA can take place at high temperature under atmospheric pressure. It will lead to the separation between MMA and polymerization inhibitor so that raising the probability of polymerization and hinder the progress of the reaction. In view of this situation, certain reaction pressure ( $>0.1 \text{ MPa}$  calculated by Aspen plus) could be utilized to guarantee the esterification system in the liquid phase among the reaction temperature range, which was certificated that pressurization can indeed enhance yield and no polymerization phenomenon had been found in a batch reactor [36]. Further, different pressures (from 0.1 to  $0.5 \text{ MPa}$ ) were applied to evaluate the situation of reaction in a fix-bed reactor

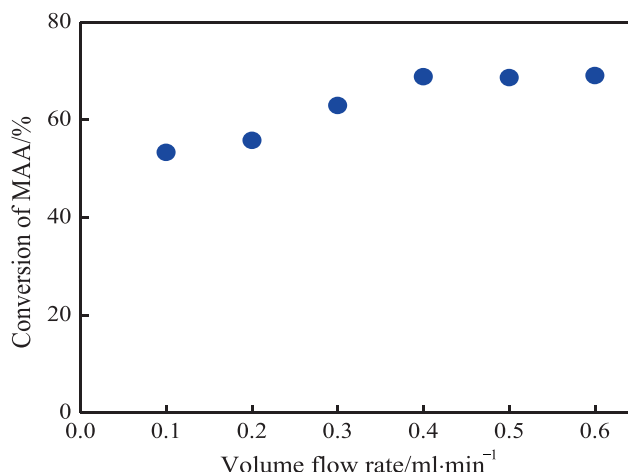


Fig. 2. Influence of the feed flow rate on the conversion of MAA at the reaction condition of MeOH/MAA = 1.0,  $0.3 \text{ MPa}$ ,  $368.15 \text{ K}$ ,  $50 \text{ ml}$  catalyst.

to compare with batch reactor results. As shown in Fig. 5, the impact of pressure to the conversion of MAA is negligible when the pressure is equal or higher than  $0.1 \text{ MPa}$  in the fixed bed reactor.

#### 3.3.3. Effect of reaction temperature

The experiments were carried out in the range of  $323.15$  to  $368.15 \text{ K}$  with the catalyst volume being  $50 \text{ ml}$ , MeOH to MAA is 1:1, and pressure of  $0.3 \text{ MPa}$ . Fig. 6 shows the conversion of MAA increased with the enhance of reaction temperature, which implies that the rate of forward reaction was favored with increase in reaction temperature. It can be considered that the molecular move faster and the intermolecular collision is more violent at high temperature, and resulting in the acceleration of bond breaking and combination [34]. However, temperature was unable to rise without limitation on account of the tolerance of resin catalyst and the situation of polymerization of the product at high temperature.

#### 3.3.4. Effect of the molar ratio of MeOH to MAA

The catalytic reaction of MAA with MeOH over NKC-9 was investigated at the temperature of  $368.15 \text{ K}$  with MeOH/MAA = 0.8, 1, 1.2 and 1.4, respectively. Fig. 7 implies that enhancing the proportion of MeOH of reactants is beneficial to improving

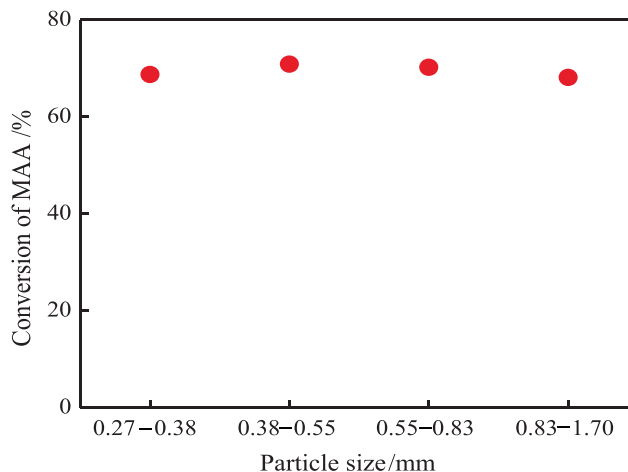


Fig. 3. Influence of the size of catalysts on the conversion of MAA at the reaction condition of MeOH/MAA = 1.0,  $0.3 \text{ MPa}$ ,  $368.15 \text{ K}$ ,  $50 \text{ ml}$  catalyst and  $0.5 \text{ ml}\cdot\text{min}^{-1}$  volume flow.

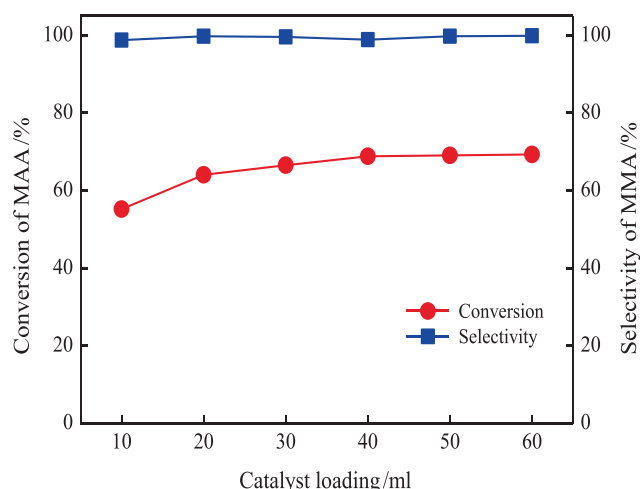


Fig. 4. Influence of the loading amount of NKC-9 on the conversion and selectivity of MAA at the reaction condition of MeOH/MAA = 1.0, 0.3 MPa, 368.15 K and 0.5 ml·min<sup>-1</sup> volume flow.

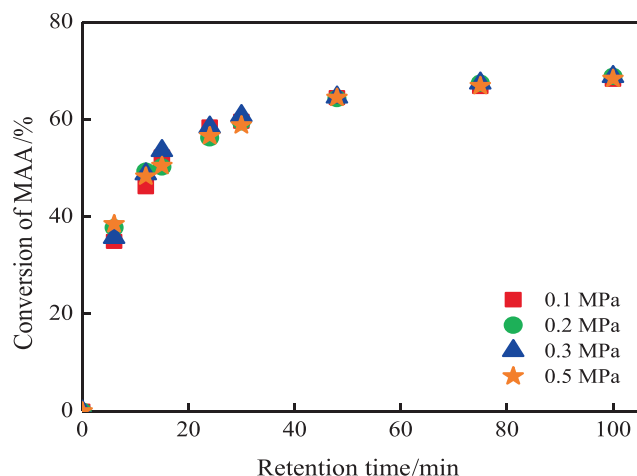


Fig. 5. Influence of reaction pressure at the reaction condition of MeOH/MAA = 1.0, 368.15 K, 50 ml catalyst and 0.5 ml·min<sup>-1</sup> volume flow.

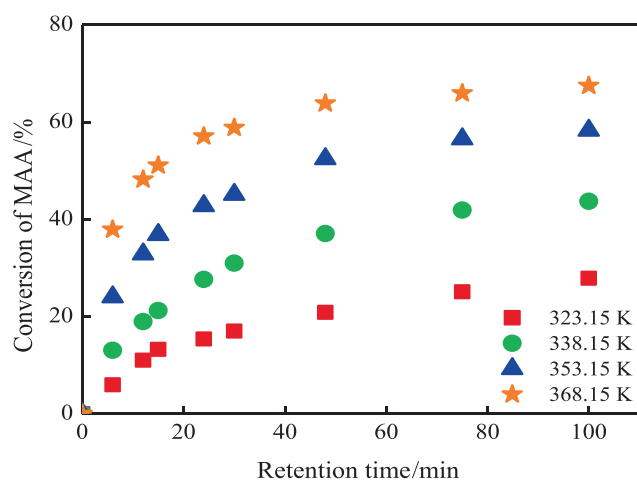


Fig. 6. Influence of reaction temperature at the reaction condition of MeOH/MAA = 1.0, 0.3 MPa, 50 ml catalyst and 0.5 ml·min<sup>-1</sup> volume flow.

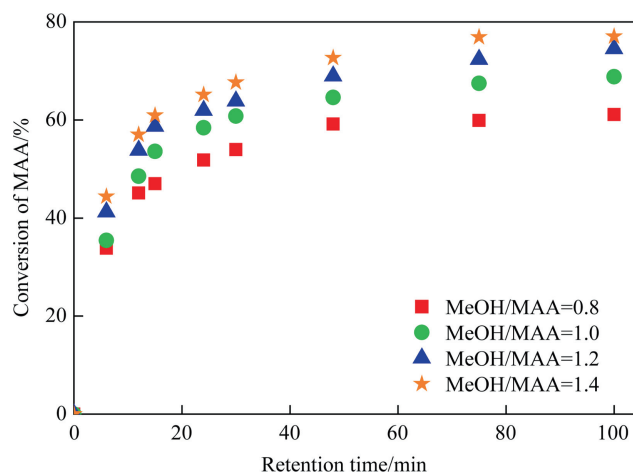
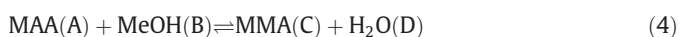


Fig. 7. Influence of the molar ratio of MeOH to MAA at the reaction condition of 0.3 MPa, 368.15 K, 50 ml catalyst and 0.5 ml·min<sup>-1</sup> volume flow.

the conversion of MAA, which leads to the enhance of the yield of MMA. A conspicuous increase in the conversion of MAA was found with the ratio of alcohol to acid increased from 0.8 to 1.2. Nevertheless, the augment of the  $X_{\text{MAA}}$  was insignificant when MeOH/MAA varied from 1.2 to 1.4. It can be considered that the active center of the catalyst surface occupied by abundant methanol molecules so that its activity no longer increases evidently [43]. In addition, the separation of methanol can be difficult in the situation of high content, which further increases the energy consumption for industrial applications [44,45]. According to the results of the experiment, the best choice of MeOH/MAA is 1.2. And the data of concentration of collected products at different MeOH/MAA molar ratio and retention time and the GC results of the liquid phase and gas phase of the reaction system are shown in Table S1 and Fig. S5. It is indicated that the amount of MeOH and MMA in the gas phase can be ignored.

### 3.4. Kinetic studies

The rate expression  $-r_A$  was determined by the assumption of the mechanism of corresponding reaction and could be described using different models including P-H, E-R and L-H. The chemical equation of the synthesis of MMA by esterification can be exhibited as follows:



where A, B, C and D are methyl acrylic, methanol, methyl methacrylate and water, respectively. Therefore, a general kinetic expression for these models could be written as:

$$-r_A = \frac{k_f(X_A X_B - X_C X_D / K_{eq})}{(1 + K_A X_A + K_B X_B + K_C X_C + K_D X_D)^n} \quad (5)$$

where  $r_A$  refers to the reaction rate in terms of mole fraction of  $i$  component;  $K_i$  is the adsorption constant of different components,  $K_{eq}$  is the reaction equilibrium constant and  $k_f$  is the forward reaction rate constant, with  $n = 0$  for the P-H model, 1 and 2 for the E-R model and the L-H model (assuming the rate-controlling step is surface reaction on the catalyst), respectively. And the specific derivation process of the L-H model could be proposed as Fig. 8:

#### 3.4.1. Reaction equilibrium constant and parameter calculation

The equilibrium constant of reaction can be calculated by Eq. (6), where  $X_{ie}$  refers to the equilibrium mole percent of each substance and the results of equilibrium conversion and thermodynamic parameters were listed in Table 3.



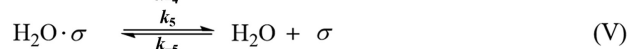
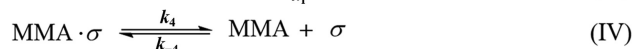
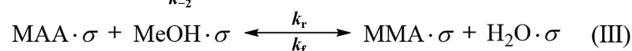
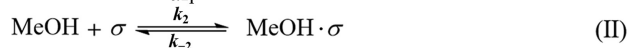


Fig. 8. Proposed the L-H mechanism of the synthesis of MMA through esterification.

$$K_{\text{eq}} = \frac{X_{\text{Ce}} \cdot X_{\text{De}}}{X_{\text{Ae}} \cdot X_{\text{Be}}} \quad (6)$$

$$\Delta G = -RT \ln K_{\text{eq}} = 75.716 \times 10^3 - 219.66T \quad (7)$$

Linear relationship of  $\ln K_{\text{eq}}$  and  $1/T$  was carried out in the light of van't Hoff equation and as shown in Fig. 9.

### 3.4.2. Modeling the adsorption experiments

An isothermal non-reactive binary adsorption experiment was applied to achieve the parameters of the adsorption equilibrium [41]. For a binary adsorption system, an overall material balance can be expressed as follows [46]:

$$\frac{n_0 \Delta x}{m} = n_1^s x_2 - n_2^s x_1 \quad (8)$$

Here on,  $n_0$  refers to the total molar number in the liquid phase,  $m$  represents the mass of NKC-9,  $\Delta x$  is the variation of the mole fraction in the liquid phase, and  $n_i^s$  is the molar mass of component  $i$  adsorbed on the surface of per unit quality of adsorbent. The composite isotherm equation was further optimized by Song *et al.* based on the above conception and as shown in Eq. (9) [41].

$$\frac{n_0 \Delta x}{m} = \frac{n^s (K_{1,2} a_1 x_2 - a_2 x_1)}{K_{1,2} a_1 + a_2} \quad (9)$$

And the ratio of the adsorption equilibrium constants of components 1 and 2 represented by  $K_{1,2}$ ,  $n^s$  delegate the total molar number of the substances attached on the adsorbent, and it can be gained directly through the fitting results of adsorption experiments with Eq. (9). Three binary non-reactive pairs including MAA with  $\text{H}_2\text{O}$  (1), MeOH with MMA (2), MeOH with  $\text{H}_2\text{O}$  (3) were performed at room temperature to determine the ratio of the adsorption equilibrium constants of MAA, MeOH, MMA to  $\text{H}_2\text{O}$ . Fig. 10(a) to (c) indicates the consequences of different binary adsorption experiments and calculated values from Eq. (9) through smooth curves. The order of adsorption intensity on the NKC-9 followed the sequence of  $\text{H}_2\text{O} > \text{MAA} > \text{MeOH} > \text{MMA}$  and relevant results were listed in Table 4. According to the calculation results, the ratio of adsorption constants of MMA: MeOH: MAA:  $\text{H}_2\text{O}$  was 0.035: 0.148: 0.237: 1. And the above data can be introduced into the model of E-R and L-H so as to reduce the quantities of unknown parameters.

Table 3  
Equilibrium conversion and thermodynamic parameters at different temperatures

Temperature/K	Equilibrium conversion/%	$K_{\text{eq}}$	$\Delta G/\text{kJ} \cdot \text{mol}^{-1}$
323.15	27.9	0.1598	4.7
338.15	43.7	0.6388	1.4
353.15	58.3	2.0904	-1.9
368.15	67.5	4.8912	-5.2

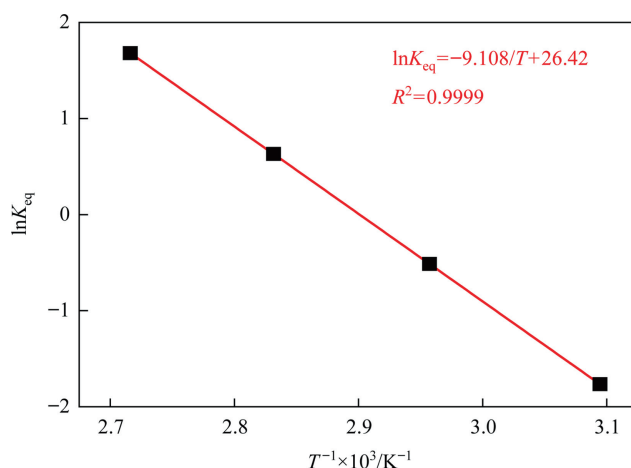


Fig. 9. Relationship between  $\ln K_{\text{eq}}$  and  $1/T$ .

The NKC-9 was impregnated in a single component to evaluate the capacity of swelling in different substances and results were exhibited in Table 5, which three times repeated measurements were conducted at least and mean values were given. Assuming that the change of volume of bed was consistent with the volumes of the individual resin microspheres and ideal mixing for the sake of facilitating to calculate the adsorbed mass, volume and amount of the unit mass of the catalyst.

### 3.4.3. Correlation of kinetic data and determination of activation energy

The relevant experimental data were regressed with three models (P-H, E-R, L-H) to ensure the kinetic and thermodynamic parameters. The fitted results were checked by the least-square method to confirm the optimal fit values and it is shown in Eq. (10).

$$\min \text{ER} = \sum \left( \frac{|n_{\text{calc},i} - n_{\text{expt},i}|}{n_{\text{expt},i}} \right) \quad (10)$$

The mass balance equation of the esterification between MeOH and MAA in a continuous reactor can be defined by Eq. (11).

$$\frac{W}{10^3 F_A} = \int_0^{x_A} \frac{dx_A}{(-r_A)} \quad (11)$$

where  $F_A$  refers to the feed flow rate of MAA,  $-r_A$  is the reaction rate of MAA and it can be obtained from the hypothesized reaction mechanism. Altering the values of the input constantly among the process of the parameter calculation so as to make sure the most appropriate results. The accuracy of the different models was validated by deviation between calculated and measured values, which consider the mean relative deviation (MRD) as the criterion and the formula is shown in Eq. (12) [34]. The correlated results and MRD based on mole fraction of three models were represented in Table 6. And the values of the exponential factor and activation carrier of each model were deduced from Arrhenius equation. The range of activation of different models was 50–60  $\text{kJ} \cdot \text{mol}^{-1}$  and it is in accordance with the experiment conditions.

$$\text{MRD} = \frac{1}{N} \left( \sum_i^N \left| \frac{x_{\text{calc},i} - x_{\text{expt},i}}{x_{\text{expt},i}} \right| \right) \times 100\% \quad (12)$$

where  $N$  refers to the quantities of data points,  $x_{\text{calc},i}$  and  $x_{\text{expt},i}$  are the mole fraction of calculated and experimental of  $i$  component, respectively.

It could be seen from Table 6 that the E-R and L-H models appear to be better than the P-H model. It is indicated that the

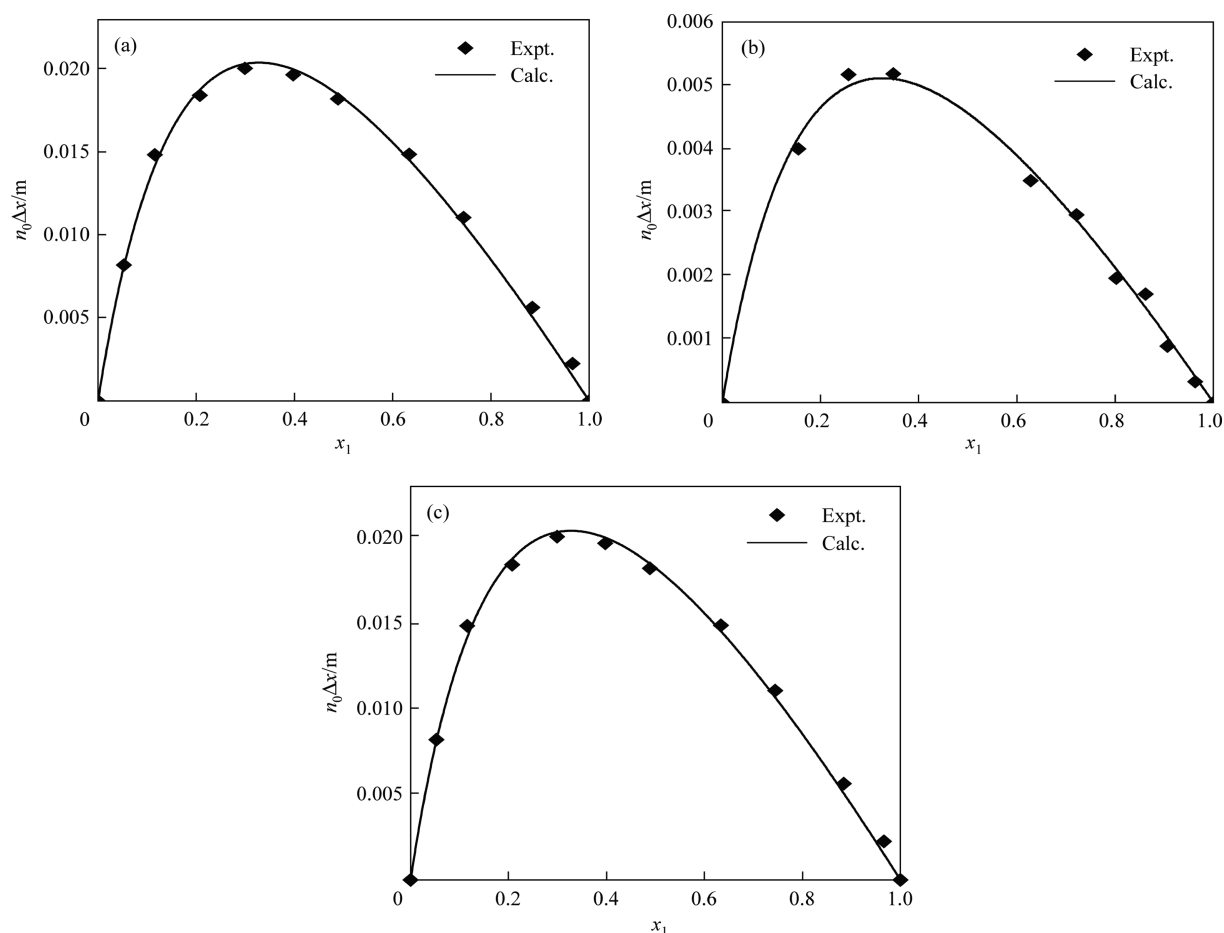


Fig. 10. Adsorption equilibrium graphs of (a) water (1) + methacrylic acid (2); (b) methanol (1) + methyl methacrylate (2); (c) water (1) + methanol (2) at room temperature on NKC-9.

**Table 4**  
Regression and calculation results of adsorption experiments

Mixture (1) + (2)	$n^S/\text{mol}\cdot\text{g}^{-1}$	$K_{1,2}$	AAD/%
Water + methacrylic acid	0.059	4.22	4.75
Water + methanol	0.004	6.75	5.26
Methanol + methyl methacrylate	0.015	4.27	7.10

Note:  $\text{AAD} = \frac{1}{N} \sum_{i=1}^N \frac{|(n_0\Delta x/m)^{\text{calc.}} - (n_0\Delta x/m)^{\text{expt.}}|}{(n_0\Delta x/m)^{\text{expt.}}} \times 100\%$ , where  $N$  refers to the number of data points.

**Table 5**  
Swelling ratio and relative parameters of NKC-9 resin for pure components

Component	Swelling ratio	Adsorbed volume/ $\text{cm}^3\cdot\text{g}^{-1}$	Adsorbed mass/ $\text{g}\cdot\text{g}^{-1}$	Adsorbed amount/ $\text{mmol}\cdot\text{g}^{-1}$
Methacrylic acid	1.123	0.187	0.979	54.349
Methanol	1.747	1.161	1.604	89.034
Methyl methacrylate	1.170	0.251	1.001	55.543
Water	1.831	1.348	1.951	108.313

kinetics behavior of the production of MMA catalyzed by NKC-9 should be considered by the adsorption effect. Among the tested models, the L-H model fitted the measured results well and the deviation was the least compared with the P-H and E-R model. The influence of temperature on the forward reaction rate constants, the Arrhenius plot for activation barriers and the pre-exponential factor were assessed by L-H mode, which can be written as Eq. (13).

**Table 6**  
Identification of forward pre-exponential factor  $A$  and activation energy  $E_a$  for three models

Model	$10^8 A$	$E_a/\text{kJ}\cdot\text{mol}^{-1}$	MRD/%
P-H	1.32	50.25	7.50
E-R	9.06	53.42	5.45
L-H	65.52	56.71	4.34

$$k_r = 6.55 \times 10^9 \exp(-6.82 \times 10^3/T) \quad (13)$$

In addition, the conclusion that the L-H model simulated results associated well with the experimental values could be drawn from Fig. 11.

### 3.5. Long period lifetime evaluation and stability research

The brilliant catalytic performance of NKC-9 had been demonstrated in a fix-bed reactor. However, the lifetime and stability of the catalyst are also an indispensable factor for industrial applications. As could be seen from Fig. 12, the NKC-9 catalyst holds the equivalent conversion of MAA and selectivity of MMA during 3000 h continuous operation, which convincingly certified the excellent stability of NKC-9. Considering that the reaction system was carried out under the nitrogen atmosphere, the heat stability of NKC-9 resin was characterized by TG-DSC under nitrogen atmosphere and as shown in Fig. 13. It implies that the weight loss below 100 °C on behalf of the evaporation of water adsorbed on the NKC-9, while the weightless peak around 210 °C could be believed as a result of the destruction of the structure of catalyst. Consequently, it can be deemed that the NKC-9 catalyst has a stable structure below 210 °C under nitrogen atmosphere, which fulfills the experimental conditions. Moreover, several characterizations were applied in order to compare the distinction and stability of new and used NKC-9 resin. Fig. 14(a) and (b) show the surface morphology of NKC-9 resin before and after use by the SEM picture with a magnification of 50000 $\times$ , it could be seen that the appearance of NKC-9 is basically unchanged after long-term operation. The XRD diagram of new and used NKC-9 resin shown in Fig. 15 were obtained from  $2\theta = 10^\circ$  to  $90^\circ$ . Three broad peaks appear in the  $2\theta$  range of  $17.8^\circ$ ,  $26.8^\circ$  and  $42.1^\circ$  belong to NKC-9. In addition, there is no variation of the catalyst before and after use exhibited on the XRD pattern [34]. Fig. 16 displays the FT-IR diagram of the NKC-9 before and after use. The characteristic peaks at  $1600\text{ cm}^{-1}$ ,  $1500\text{ cm}^{-1}$  and  $1450\text{ cm}^{-1}$  could be regarded as the vibration of the skeleton of the benzene ring. The presence of the sulfonic groups could be confirmed by the peaks at  $1008\text{ cm}^{-1}$  and  $908\text{ cm}^{-1}$ . According to the graph, the main peaks in the FT-IR of new and used NKC-9 were practically identical. Besides, the hydrogen ion concentration (total acidity) of the catalyst before and after use were 4.09 and 3.99  $\text{mmol}\cdot\text{g}^{-1}$  via element analysis [25]. And the relevant results are shown in Supplementary Material. In summary, NKC-9 catalyst exhibited outstanding stability in the reaction of esterification to synthesize MMA.

## 4. Conclusions

In this work, the synthesis of MMA through esterification on different resin catalysts was investigated in a fixed-bed reactor. It can be found that the NKC-9 catalyst has the outstanding catalytic activity and stability in the continuous reaction. The optimal reaction condition is MeOH/MAA is 1.2, reaction temperature is 368.15 K and relative pressure of 0.3 MPa. It is revealed that the sequence of adsorption equilibrium constants of components followed the order of  $\text{H}_2\text{O} > \text{MAA} > \text{MeOH} > \text{MMA}$  via the adsorption experiments. The fitting results of L-H model were the best of the three models and the activation energy is  $56.7\text{ kJ}\cdot\text{mol}^{-1}$ , which can be further used to predict the distillation and simulation of the esterification system of MAA with MeOH in industrial production. Based on the above experiments, NKC-9 can be a promising candidate for the industrial production of MMA.

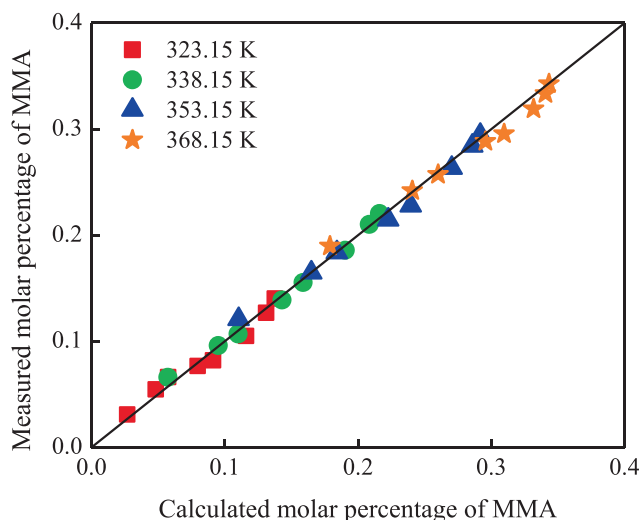


Fig. 11. Comparison of the calculated results with experimental data recorded at the condition of MeOH/MAA = 1.0, 0.3 MPa, 50 ml catalyst and  $0.5\text{ ml}\cdot\text{min}^{-1}$  volume flow.

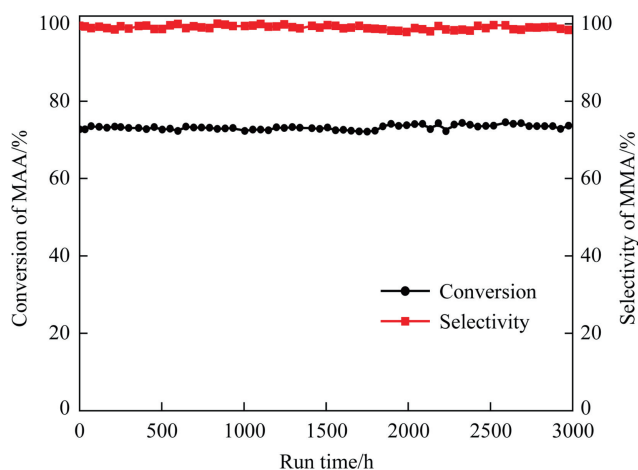


Fig. 12. Lifetime evaluation of NKC-9 resin.

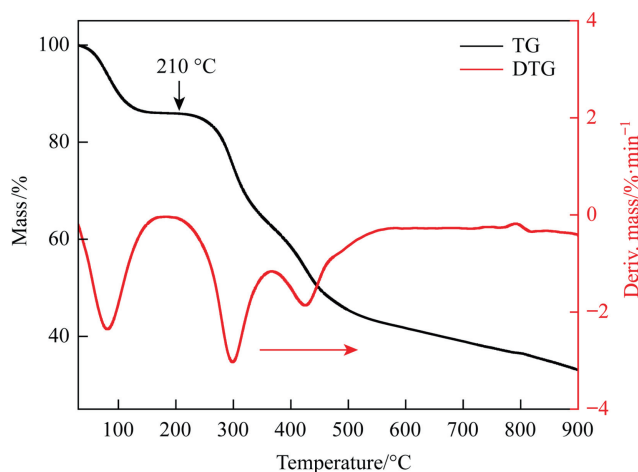


Fig. 13. TG analysis for NKC-9 catalyst.



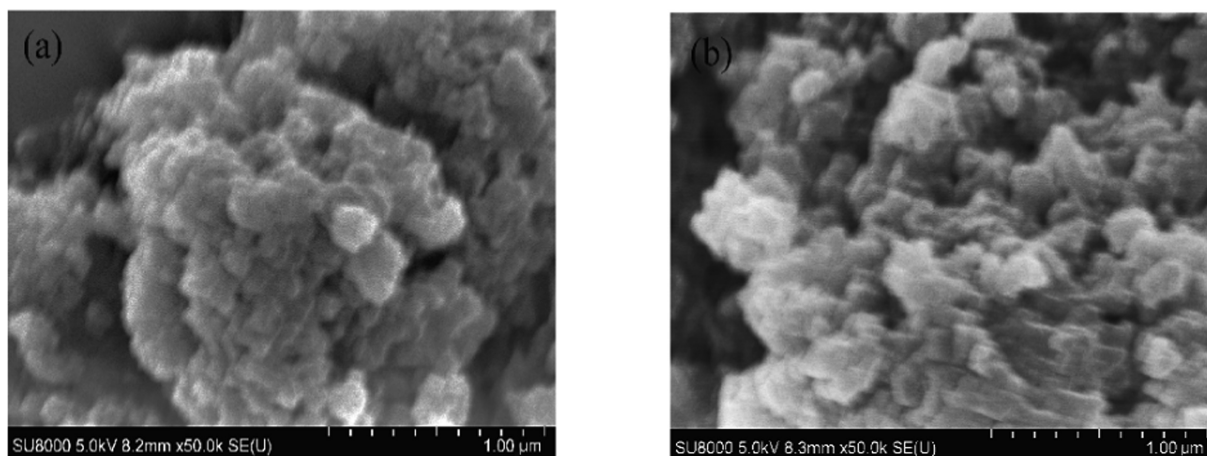


Fig. 14. SEM images of fresh NKC-9 (a) and used NKC-9 (b) with a magnification of 50000 $\times$ .

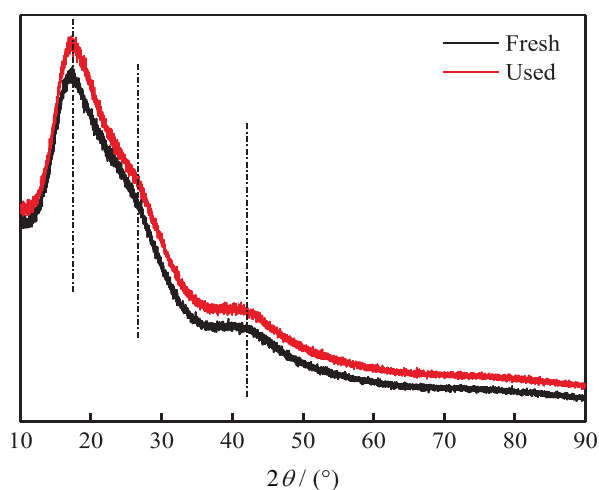


Fig. 15. XRD patterns of the fresh and used NKC-9 catalyst.

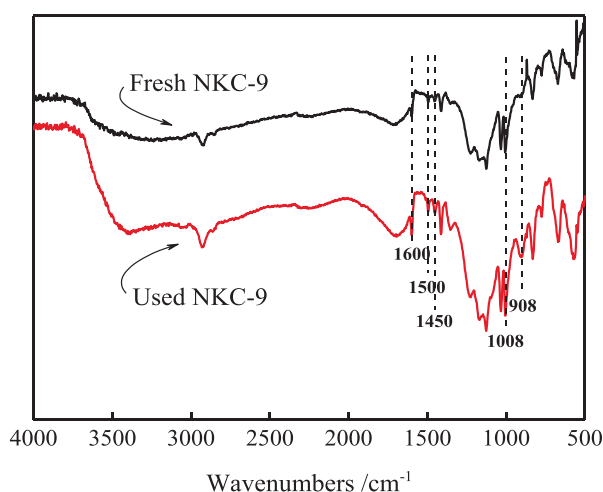


Fig. 16. IR spectra of the NKC-9 before and after use.

### Declaration of Competing Interest

The authors declare that they have no known competing financial interests or personal relationships that could have appeared to influence the work reported in this paper.

### Acknowledgements

For this study, we would like to express the gratitude to the National Natural Science Fund for Distinguished Young Scholars (22025803). It was supported by the National Natural Science Foundation of China (22178338), the Joint Fund of the Yulin University and the Dalian National Laboratory for Clean Energy (YLU-DNL Fund 2021018). Likewise, and we would thank to the financial support of project “Research and development and industrial application of new catalytic materials for green synthesis of MMA to replace highly toxic HCN” (Hebei, 20374002D).

### Supplementary Material

Supplementary data to this article can be found online at <https://doi.org/10.1016/j.cjche.2022.10.011>.

### Nomenclature

$A$	pre-exponential factor
$a_i$	activity of $i$
$E_a$	activation energy, $\text{kJ}\cdot\text{mol}^{-1}$
$F$	volume flow rate, $\text{ml}\cdot\text{min}^{-1}$
$\Delta G$	Gibbs free energy, $\text{kJ}\cdot\text{mol}^{-1}$
$K_{a,b}$	ratio of the adsorption equilibrium constants of a to b
$K_{eq}$	reaction equilibrium constant
$K_i$	adsorption equilibrium constant
$k_r$	reaction rate constant
$N$	number of experimental points
$n$	number of mole number of $i$ adsorbed on the adsorbent, mol
$n_{calc,i}$	mole number of $i$ calculated by model, mol
$n_{expt,i}$	mole number of $i$ measured by experiment, mol
$n_{i,0}$	molar number of $i$ at the beginning, mol
$n_{i,t}$	molar number of $i$ after $t$ time, mol
$n^S$	total molar number of the absorbed compound for adsorbent, mol
$n_0$	total initial number of moles, mol
$r$	reaction rate, $\text{mol}\cdot\text{g}^{-1}\cdot\text{min}^{-1}$
$R$	universal gas constant, $\text{J}\cdot\text{mol}^{-1}\cdot\text{K}^{-1}$
$S_i$	selectivity of $i$ , %
$T$	temperature, K
$V$	catalyst packing volume, ml
$X_i$	conversion of $i$ , %
$X_{ie}$	equilibrium mole fraction of $i$ , %
$x_{calc,i}$	mole fraction number of $i$ calculated by model, %
$x_{expt,i}$	mole fraction number of $i$ measured by experiment, %

$x_i$	molar fraction of $i$ , %
$\Delta x$	amount of change in the mole fraction, mol
$\tau$	retention time, $\text{min}^{-1}$

## References

- [1] K. Nagai, New developments in the production of methyl methacrylate, *Appl. Catal. A Gen.* 221 (1–2) (2001) 367–377.
- [2] A. Hariilal, V.D.B.C. Dasireddy, H.B. Friedrich, Effect of water and methanol in the production of methyl methacrylate over iron phosphate catalysts, *React. Kinetics Mech. Catal.* 124 (1) (2018) 265–277.
- [3] M.J.D. Mahboub, J.L. Dubois, F. Cavani, M. Rostamizadeh, G.S. Patience, Catalysis for the synthesis of methacrylic acid and methyl methacrylate, *Chem. Soc. Rev.* 47 (20) (2018) 7703–7738.
- [4] U. Ali, K.J.B.A. Karim, N.A. Buang, A review of the properties and applications of poly (methyl methacrylate) (PMMA), *Polym. Rev.* 55 (4) (2015) 678–705.
- [5] B.A. Bhanvase, D.V. Pinjari, P.R. Gogate, S.H. Sonawane, A.B. Pandit, Synthesis of exfoliated poly(styrene-co-methyl methacrylate)/montmorillonite nanocomposite using ultrasound assisted *in situ* emulsion copolymerization, *Chem. Eng. J.* 181–182 (2012) 770–778.
- [6] B. Li, R.Y. Yan, L. Wang, Y.Y. Diao, Z.X. Li, S.J. Zhang, Synthesis of methyl methacrylate by aldol condensation of methyl propionate with formaldehyde over acid–base bifunctional catalysts, *Catal. Lett.* 143 (8) (2013) 829–838.
- [7] Y.N. Guan, H.X. Ma, W.Y. Chen, M.S. Li, G. Qian, D. Chen, X.G. Zhou, X.Z. Duan, Methyl methacrylate synthesis: Thermodynamic analysis for oxidative esterification of methacrolein and aldol condensation of methyl acetate, *Ind. Eng. Chem. Res.* 59 (2020) 17408–17416.
- [8] B.H. Wang, W.J. Sun, J. Zhu, W.L. Ran, S. Chen, Pd–Pb/SDB bimetallic catalysts for the direct oxidative esterification of methacrolein to methyl methacrylate, *Ind. Eng. Chem. Res.* 51 (46) (2012) 15004–15010.
- [9] Y.N. Wang, R.Y. Yan, Z.P. Lv, H. Wang, L. Wang, Z.X. Li, S.J. Zhang, Lanthanum and cesium-loaded SBA-15 catalysts for MMA synthesis by aldol condensation of methyl propionate and formaldehyde, *Catal. Lett.* 146 (9) (2016) 1808–1818.
- [10] B. Li, R.Y. Yan, L. Wang, Y.Y. Diao, Z.X. Li, S.J. Zhang, SBA-15 supported cesium catalyst for methyl methacrylate synthesis via condensation of methyl propionate with formaldehyde, *Ind. Eng. Chem. Res.* 53 (4) (2014) 1386–1394.
- [11] H.E. Hoydonckx, D.E. de Vos, S.A. Chavan, P.A. Jacobs, Esterification and transesterification of renewable chemicals, *Top. Catal.* 27 (1–4) (2004) 83–96.
- [12] H. Zhao, R. Ran, L. Wang, C.S. Li, S.J. Zhang, Novel continuous process for methacrolein production in numerous droplet reactors, *AIChE J.* 66 (7) (2020) e16239.
- [13] B.H. Wang, H. Li, J. Zhu, W.J. Sun, S. Chen, Preparation and characterization of mono-/ multi-metallic hydrophobic catalysts for the oxidative esterification of methacrolein to methyl methacrylate, *J. Mol. Catal. A Chem.* 379 (2013) 322–326.
- [14] G. Jyoti, A. Keshav, J. Anandkumar, Esterification of acrylic acid with ethanol using pervaporation membrane reactor, *Korean J. Chem. Eng.* 34 (6) (2017) 1661–1668.
- [15] D.S. Zhao, M.S. Liu, J. Zhang, J.P. Li, P.B. Ren, Synthesis, characterization, and properties of imidazole dicationic ionic liquids and their application in esterification, *Chem. Eng. J.* 221 (2013) 99–104.
- [16] J.Z. Gui, X.H. Cong, D. Liu, X.T. Zhang, Z.D. Hu, Z.L. Sun, Novel Brønsted acidic ionic liquid as efficient and reusable catalyst system for esterification, *Catal. Commun.* 5 (9) (2004) 473–477.
- [17] D. Fang, X.L. Zhou, Z.W. Ye, Z.L. Liu, Brønsted acidic ionic liquids and their use as dual solvent–catalysts for Fischer esterifications, *Ind. Eng. Chem. Res.* 45 (24) (2006) 7982–7984.
- [18] X.F. Liu, Y.W. Zhao, Z. Li, J. Chen, C.G. Xia, ChemInform abstract: Pyrrolidine-based dicationic acidic ionic liquids: efficient and recyclable catalysts for esterifications, *ChemInform* 42 (9) (2011) 2003–2008.
- [19] J. Bedard, H. Chiang, A. Bhan, Kinetics and mechanism of acetic acid esterification with ethanol on zeolites, *J. Catal.* 290 (2012) 210–219.
- [20] L. Zatta, L.P. Ramos, F. Wypych, Acid-activated montmorillonites as heterogeneous catalysts for the esterification of lauric acid with methanol, *Appl. Clay Sci.* 80–81 (2013) 236–244.
- [21] C. Huang, C.J. Yang, P. Gao, N.Q. Wang, C. Chen, J. Chang, Characterization of an alkaline earth metal-doped solid superacid and its activity for the esterification of oleic acid with methanol, *Green Chem.* 17 (2015) 3609–3620.
- [22] G. Wang, L.Y. Tao, X. Hou, H.D. Cao, C. Dong, W. Nie, J. Xu, L.Q. Zhang, Preparation, characterization of superacid  $\text{SO}_4^{2-}/\text{ZrO}_2\text{-SiO}_2$  and its activity on catalytic synthesis of methyl *p*-nitrobenzoate, *J. Wuhan Univ. Technol. Mater Sci Ed* 29 (5) (2014) 895–899.
- [23] J. Zhang, S.J. Zhang, J.X. Han, Y.H. Hu, R.Y. Yan, Uniform acid poly ionic liquid-based large particle and its catalytic application in esterification reaction, *Chem. Eng. J.* 271 (2015) 269–275.
- [24] M.J. Lee, H.T. Wu, H.M. Lin, Kinetics of catalytic esterification of acetic acid and amyl alcohol over dowex, *Ind. Eng. Chem. Res.* 39 (11) (2000) 4094–4099.
- [25] C.C. Zuo, L.S. Pan, S.S. Cao, C.S. Li, S.J. Zhang, Catalysts, kinetics, and reactive distillation for methyl acetate synthesis, *Ind. Eng. Chem. Res.* 53 (26) (2014) 10540–10548.
- [26] M. Kuzminska, R. Backov, E.M. Gagneaux, Behavior of cation-exchange resins employed as heterogeneous catalysts for esterification of oleic acid with trimethylolpropane, *Appl. Catal. A Gen.* 504 (2015) 11–16.
- [27] L.L. Ma, Y. Han, K.A. Sun, J. Lu, J.C. Ding, Kinetic and thermodynamic studies of the esterification of acidified oil catalyzed by sulfonated cation exchange resin, *J. Energy Chem.* 24 (4) (2015) 456–462.
- [28] C.R. Khudsange, K.L. Wasewar, Kinetic study of liquid phase esterification of lactic acid with *n*-amyl alcohol catalyzed by cation exchange resins: Experimental and statistical modeling, *React. Kinetics Mech. Catal.* 125 (2) (2018) 535–554.
- [29] Y.T. Tsai, H.M. Lin, M.J. Lee, Kinetics behavior of esterification of acetic acid with methanol over amberlyst 36, *Chem. Eng. J.* 171 (3) (2011) 1367–1372.
- [30] J. Hu, Q. Zhang, C. He, Q.L. Chen, Z.W. Qi, Q.G. Li, B.J. Zhang, A multi-stage activated carbon impregnation system: Isotherms, kinetics and multi-objective modeling optimization, *Chem. Eng. Sci.* 227 (2020) 115895.
- [31] M. Sharma, R.K. Wanchoo, A.P. Toor, Adsorption and kinetic parameters for synthesis of methyl nonanoate over heterogeneous catalysts, *Ind. Eng. Chem. Res.* 51 (44) (2012) 14367–14375.
- [32] H.T.R. Teo, B. Saha, Heterogeneous catalyzed esterification of acetic acid with isoamyl alcohol: Kinetic studies, *J. Catal.* 228 (1) (2004) 174–182.
- [33] W. Osorio-Viana, M. Duque-Bernal, J. Fontalvo, I. Dobrosz-Gómez, M.Á. Gómez-García, Kinetic study on the catalytic esterification of acetic acid with isoamyl alcohol over Amberlite IR-120, *Chem. Eng. Sci.* 101 (2013) 755–763.
- [34] C.C. Zuo, T.T. Ge, C.S. Li, S.S. Cao, S.J. Zhang, Kinetic and reactive distillation for acrylic acid synthesis via transesterification, *Ind. Eng. Chem. Res.* 55 (30) (2016) 8281–8291.
- [35] G. Wang, G.M. Cai, Cooperative catalytic effects between Brønsted and Lewis acid sites and kinetics for production of methyl methacrylate on  $\text{SO}_4^{2-}/\text{TiO}_2\text{-SiO}_2$ , *Chem. Eng. Sci.* 229 (2021) 116165.
- [36] R. Ran, J. Li, G. Wang, Z.X. Li, C.S. Li, Esterification of methacrylic acid with methanol: Process optimization, kinetic modeling, and reactive distillation, *Ind. Eng. Chem. Res.* 58 (6) (2019) 2135–2145.
- [37] G.D. Yang, S. Chen, X.B. Li, C.Z. Liu, J. He, W.P. Ding, Z. Zhou, Z.B. Zhang, Study on methyl esterification of salicylic acid using an intensified fixed bed reactor, *Int. J. Chem. React. Eng.* 17 (8) (2019) 20180210.
- [38] Y. Cheng, Y.H. Feng, Y.B. Ren, X. Liu, A.R. Gao, B.Q. He, F. Yan, J.X. Li, Comprehensive kinetic studies of acidic oil continuous esterification by cation-exchange resin in fixed bed reactors, *Bioresour. Technol.* 113 (2012) 65–72.
- [39] V. Russo, R. Tesser, C. Rossano, T. Cogliano, R. Vitiello, S. Leveneur, M. di Serio, Kinetic study of Amberlite IR120 catalyzed acid esterification of levulinic acid with ethanol: From batch to continuous operation, *Chem. Eng. J.* 401 (2020) 126126.
- [40] L. Chen, Y. Liu, Z. Cao, G.D. Yang, A.D. Zhou, Z. Zhou, Thermodynamic and kinetic study on the catalysis of isoamyl acetate by a cation-exchange resin in an intensified fixed-bed reactor, *ACS Omega* 5 (40) (2020) 25810–25818.
- [41] W. Song, G. Venimadhavan, J.M. Manning, M.F. Malone, M.F. Doherty, Measurement of residue curve maps and heterogeneous kinetics in methyl acetate synthesis, *Ind. Eng. Chem. Res.* 37 (5) (1998) 1917–1928.
- [42] Y.T. Tsai, H.M. Lin, M.J. Lee, Kinetics of catalytic esterification of propionic acid with methanol over amberlyst 36, *Ind. Eng. Chem. Res.* 50 (3) (2011) 1171–1176.
- [43] M.T. Sanz, R. Murga, S. Beltrán, J.L. Cabezas, J. Coca, Autocatalyzed and ion-exchange-resin-catalyzed esterification kinetics of lactic acid with methanol, *Ind. Eng. Chem. Res.* 41 (3) (2002) 512–517.
- [44] L.W. Tong, L.F. Chen, Y.M. Ye, Z.W. Qi, Analysis of intensification mechanism of auxiliary reaction on reactive distillation: Methyl acetate hydrolysis process as example, *Chem. Eng. Sci.* 106 (2014) 190–197.
- [45] R.Z. Wang, H. Qin, J.W. Wang, H.Y. Cheng, L.F. Chen, Z.W. Qi, Reactive extraction for intensifying 2-ethylhexyl acrylate synthesis using deep eutectic solvent[Im: 2PTSA, *Green Energy Environ.* 6 (3) (2021) 405–412.
- [46] J.J. Kipling, Adsorption From Solutions of Non-electrolytes, Academic Press, Beijing, 1965.